Physics Letters B 843 (2023) 137989

Contents lists available at ScienceDirect

Physics Letters B

journal homepage: www.elsevier.com/locate/physletb

# A new approach to nuclear level densities: The QRPA plus boson expansion

S. Hilaire [a,b,*], S. Goriely [c], S. Péru [a,b], G. Gosselin [a,b]

[a] CEA, DAM, DIF, F-91297 Arpajon, France
[b] Université Paris-Saclay, CEA, LMCE, 91680 Bruyères-le-Châtel, France
[c] Institut d'Astronomie et d'Astrophysique, Université Libre de Bruxelles, Campus de la Plaine CP 226, 1050 Brussels, Belgium

ARTICLE INFO

*Article history:*
Received 15 April 2023
Received in revised form 26 May 2023
Accepted 26 May 2023
Available online 1 June 2023
Editor: B. Balantekin

*Keywords:*
Nuclear level density
QRPA boson
$(n, \gamma)$ cross section

ABSTRACT

Nuclear level densities play a key role in many nuclear applications. To go beyond the usual particle-independent approximation, a conceptually new approach based on the boson expansion of QRPA excitations is proposed. The calculated nuclear level densities are shown to follow an energy dependence close to a constant-temperature formula at energies above a few MeV, but present a rather narrow spin distribution. They are shown to provide a quite remarkable agreement with s-wave resonance spacings and Oslo data, at least for the 48 even-even nuclei considered in the present study.



## 1. Introduction

The knowledge of nuclear level densities (NLDs) plays a key role in the evaluation of the nuclear data and in many nuclear applications. It has been a field of research for years going back at least to 1936 with Bethe's pioneering work [1]. Based on the corresponding Fermi Gas model, a large number of analytical formulas have been proposed to describe not only the exponential increase of levels with excitation energies, but also the impact of shell, pairing and collective effects (see, e.g. Ref. [2] and references therein).

Level densities play a key role for modelling nuclear reactions. With the development of new facilities and innovative experiments, as well as for astrophysical purposes, nuclear data far from the valley of stability are required. This challenges the NLD models. Indeed, cross section predictions have mainly relied on more or less phenomenological approaches, depending on parameters adjusted to scarce experimental data or deduced from systematics. Such predictions are expected to be reliable for nuclei not too far from experimentally accessible regions, but are questionable when dealing with exotic nuclei. To face such difficulties, it is preferable to rely on as fundamental (microscopic) as possible methods based on physically sound models.

Microscopic models of NLD have been developed (see e.g. [3–9] and references therein), but they are seldom used for practical applications due to (*i*) their lack of accuracy in reproducing experimental data (especially when considered globally on a large data set), (*ii*) their restricted flexibility in comparison with highly parametrized analytical expressions, or (*iii*) their limitation when applied to the large set of nuclei needed for applications. The combinatorial approach followed in Refs. [3,4] clearly demonstrated that such models can compete with the statistical ones in the global reproduction of experimental data. This approach provides energy, spin and parity dependence of NLD, and, at low energies, describes the non-statistical limit which, by definition cannot be described by the traditional statistical formulas. Such a non-statistical behaviour can have a significant impact on cross section predictions, particularly when calculating cross sections known to be sensitive to spin or parity distributions such as for isomeric production or low-energy neutron capture [10]. However, the combinatorial method also offers room for improvement because of the phenomenological aspects of some ingredients it contains as well as the fundamental assumption of independent particles it entails, as all statistical approach also do; both aspects could hamper its microscopic nature, and consequently its predictive power, especially at the lowest energies.

When considering publicly available global NLD models providing predictions for a large number of nuclei, only a limited number of methods are available. These include one of the many analytical forms of the Fermi Gas model [see e.g 2,11], the statistical model based on mean-field single-particle scheme and pairing properties [12] and the combinatorial approach [3,4]. Such a collection of NLD models is in particular available in the TALYS

* Corresponding author at: CEA, DAM, DIF, F-91297 Arpajon, France.
*E-mail address:* stephane.hilaire@cea.fr (S. Hilaire).

https://doi.org/10.1016/j.physletb.2023.137989

reaction code [13,14]. All these models more or less reproduce equally well the overall set of NLD experimental data that essentially consist of low-lying levels, s-wave resonance spacings at the neutron separation energy [2] and the Oslo data [15,16]. They are all based on the independent-particle approximation, so that at energies below a few MeV, they all failed to reproduce the detailed structure-dependent distribution of low-lying levels, in particular the vibrational ones. More microscopic approaches, like the shell model and its many variants, include correlations beyond mean-field theory but their applications, even within the shell model Monte Carlo method [7,8], are restricted to medium-mass nuclei and can hardly be extended to the thousands of nuclei of interest in nuclear applications.

For this reason, a conceptually new approach beyond the independent-particle approximation and still tractable at large scale is proposed here on the basis of the boson expansion of QRPA excitations (hereafter referred to as QRPA+BE). After describing the methodology, the energy, parity and spin distributions of the newly estimated NLDs are compared with other global models and available experimental data.

## 2. Methodology

### 2.1. Building QRPA excitations

Considering the underlying quasi-boson approximation, all QRPA states are boson excitations acting on the QRPA vacuum. The latter can be built from the HFB ground state with an exponential form of boson operators (see e.g. Eq. 8.101 of [17]). Such a QRPA formalism based on axially-symmetric-deformed HFB equations solved in a finite harmonic oscillator basis in cylindrical coordinates has been described in details in Refs. [18–23]. This QRPA method using the D1M Gogny force [24] has proven its capacity to predict the E1 and M1 photon strength functions [21,25] as well as the Gamow-Teller response [26,23] with a high degree of reliability. The QRPA method has also shown its capacity to reproduce rather well low-lying vibrational levels [20,25]. In the present study, the D1M+QRPA approach is used to estimate all intrinsic states with angular momentum projection up to $K_{\max} = 9$.

The impact of the size of the basis dimension and two-quasi-particle excitation energy cutoff on the $K = 0^-$ and $K = 1^-$ strengths and energies has been studied in Ref. [21] and will not be re-iterated here. Note, however, that for nuclei up to $Z = 74$, QRPA calculations are performed without any energy cutoff on the two-quasi-particle states energies. In contrast, for $Z \geq 76$ nuclei, a cutoff energy $\varepsilon_c = 120$ MeV is applied for practical consideration, *i.e.* to decrease the computational time. Since for heavy systems like actinides, it remains computerwise extremely heavy to consider large basis dimension and large cutoff energies of the two-quasi-particle states, nuclei with $Z > 82$ are not considered at this stage.

### 2.2. The boson expansion

To go beyond the QRPA excitations, the level density can be properly described using a boson partition function [27]. The construction of the intrinsic plus vibrational states consists in expanding the generalized boson partition function,

$$\mathcal{Z}_{\text{boson}} = \prod_{\lambda} \prod_{\mu=-\lambda}^{\lambda} \sum_{N_{\text{boson}}} \left[ y^{\varepsilon_{\lambda\mu}} t^{\mu} p_{\lambda} \right]^{N_{\text{boson}}} , \tag{1}$$

where $y$, $t$ and $p$ keep track of the boson excitation energies, their spin and parity projections, respectively. In this equation, $\varepsilon_{\lambda\mu}$ is the energy of a QRPA boson with multipolarity $\lambda$ and spin projection $\mu$, and $p_\lambda = (-1)^\lambda$ or $(-1)^{(\lambda+1)}$ for magnetic and electric excitations, respectively. The expansion of Eq. (1) formally yields a polynomial form in which the coefficient $C(U, M)$ before the term $y^U t^M$, for a given parity $\pi$, corresponds to the number of ways one can couple bosons for a given total excitation energy $U$ and angular momentum projection $M$. Matrix algebra, as described in Refs. [27,28], enables the total parity assignment. Dividing $C(U, M)$ by the width of the discretized bin provides the total state density in the laboratory frame, i.e. $\omega_{tot}(U, M, \pi)$ [3,27,28]. All details relative to Eq. (1) can be found in Ref. [27]. However, it should be emphasized that the present approach is conceptually different from our previous works [27,28,3]. There is no need to perform here any convolution with incoherent particle-hole excitations, since those are implicitly included in the QRPA phonons. In addition, there is no limit on the number of phonons included in Eq. (1).

### 2.3. Spurious and unphysical states

Although the QRPA calculations described above are performed without any energy cut-off (at least for $Z \leq 74$ nuclei), some spurious states within various $K^\pi$ blocks may be predicted with a non-zero energy (though without perturbing the rest of the spectrum) [20] and consequently needs to be omitted. More specifically,

- $K^\pi = 0^+$: due to pairing interaction for neutron or protons, the first or first two $K^\pi = 0^+$ modes may be spurious for non-zero neutron and/or proton pairing and should not be included in the boson expansion;
- $K^\pi = 1^+$: for deformed nuclei, a rotation perpendicular to the symmetry axis may lead to a spurious first $1^+$ that needs to be excluded;
- $K^\pi = 0^-/1^-$: translational invariance should bring the first $0^-$ and $1^-$ energies down to zero, but, if not, such a spurious state should be removed.

In addition, some low-lying $K^\pi = 2^+$ states may also be unphysical. In particular, in the case of triaxial deformed or $\gamma$-soft nuclei calculated within the axial approximation, the first $2^+$ state may be found artificially too low, giving rise to an increase of NLD. This pathology is avoided by constraining the energy of the lowest $2^+$ state to a value at least higher than $E^{\min}_{2^+} = 40\ A^{-5/6}$ MeV, as extracted from experimental data [28].

Finally note that in addition to the presence of spurious states, QRPA excitation energies with D1M or D1S interactions tend to be overestimated (see Fig. 1 of Ref. [25]) by typically 100-200 keV. For this reason, all QRPA $K^\pi$ energies are lowered here by 150 keV before applying the boson expansion. Similarly, the D1M interaction is known to give rather strong shell effects due to its low effective mass leading to a systematic overestimate of QRPA excitations for closed shell nuclei. We find in particular that the first $^{208}$Pb $2^+$ and $3^-$ levels are overestimated by typically 0.6 MeV. By simplicity for nuclei with $Z$, $N$ or $N + 2$ corresponding to magic numbers, a constant energy shift of -0.65 MeV has been applied to all $K^\pi$ components. The impact of such an empirical correction is discussed below.

## 3. The QRPA+BE level densities

For spherical nuclei, the level density can be estimated from

$$\rho_s(U, J, \pi) = \omega_{\text{tot}}(U, M = J, \pi) - \omega_{\text{tot}}(U, M = J + 1, \pi), \tag{2}$$

while for deformed nuclei, rotational bands need to be constructed, so that the NLD reads [28,6]

$$\rho_{\rm d}(U,J,\pi)=\frac{1}{2}\left[\sum_{K=-J,K\neq 0}^{J}\omega_{\rm tot}(U-E_{rot}^{J,K},K,\pi)\right]$$
$$+\omega_{\rm tot}(U-E_{rot}^{J,0},0,\pi)\Big[\delta_{(J\,even)}\,\delta_{(\pi=+)}$$
$$+\delta_{(J\,odd)}\,\delta_{(\pi=-)}\Big]. \quad (3)$$

In Eq. (3), the symbol $\delta_{(x)}$ (defined by $\delta_{(x)}=1$ if $x$ holds true and 0 otherwise) restricts the rotational bands built on intrinsic states with spin projection $K=0$ and parity $\pi$ to the levels sequences0, 2, 4, ... for $\pi=+$ and 1, 3, 5, ... for $\pi=-$. Finally, the rotational energy is obtained with the well-known expression [29],

$$E_{rot}^{J,K}=\frac{J(J+1)-K^2}{2\mathcal{J}_\perp}, \quad (4)$$

where $\mathcal{J}_\perp$ is the Belyaev moment of inertia of a nucleus rotating around an axis perpendicular to the symmetry axis, as determined within the HFB approach with D1M effective interaction. The Belyaev moment of inertia is typically about 30% lower than experimental one and is consequently systematically increased by 30% in the present calculations.

Finally, it is well known that there is a sharp transition appearing when selecting either Eq. (2) or (3) (i.e. if a nucleus is spherical or deformed). Both spherical and well-deformed nuclei can be properly described in the present framework. However, it fails to describe intermediate cases for which an exact projection technique should be included. For this reason, to smooth out the difficult cases of transitional deformation, a phenomenological damping function $\mathcal{F}$ is introduced [3,28] such that

$$\rho(U,J,\pi)=\Big[1-\mathcal{F}\Big]\rho_s(U,J,\pi)+\mathcal{F}\rho_d(U,J,\pi). \quad (5)$$

We consider, as in Ref. [4], an expression depending on the quadrupole deformation parameter $\beta_2$ only which reads

$$\mathcal{F}=1-\Big[1+{\rm e}^{(\beta_2-0.18)/0.04}\Big]^{-1}, \quad (6)$$

where the parameters have been adjusted in order to reproduce at best the measured s-wave mean spacings.

### 3.1. Energy distribution

The energy dependence of the QRPA+BE NLD (for both parities) is compared for the spherical $^{136}$Ba and deformed $^{170}$Yb nuclei in Fig. 1 with 2 alternative and widely used NLD models, namely the HFB plus combinatorial (HFB+comb) [3] and the constant temperature (Cst-T) matched to the Fermi gas model [11]. Above a few MeV, the QRPA+BE NLD is found to give an energy dependence rather similar to the Cst-T one, both for the spherical and deformed nuclei. Deviations from a simple exponential law are however found at low energies and depict the complex nuclear structure properties of each individual case.

### 3.2. Parity distribution

The parity-dependent QRPA+BE NLDs are also compared in Fig. 1. As observed, the equiparity is seen to require a higher excitation energy in the QRPA+BE case than in the particle-independent combinatorial approach. In particular, an energy of more than 10 MeV is needed to reach the equiparity. For deformed nuclei, the equiparity is achieved above $\sim 2$ MeV, but also at energies relatively higher than in the HFB+comb approach.

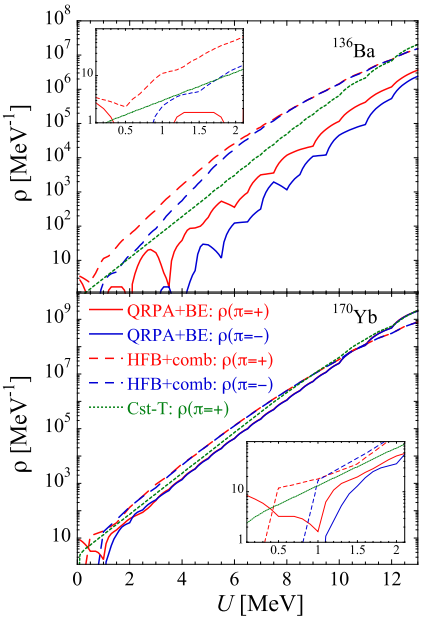


**Fig. 1.** Total parity-dependent NLD of $^{136}$Ba and $^{170}$Yb as a function of the excitation energy $U$ for 3 different models, including the present QRPA+BE (solid lines), HFB+comb [3] (dashed lines), and the Cst-T [11] (dotted line). Positive- (negative-) parity NLD are given in red (blue). The Cst-T model assumes equiparity. The inserts in both panels emphasise the non-Cst-T behaviour of the QRPA+BE NLD at low energies.

### 3.3. Spin distribution

The spin distribution of the QRPA+BE NLD is illustrated in Fig. 2 for a spherical and a deformed nucleus at 5 different energies ranging between 4 and 12 MeV. These spin distributions are also compared with the HFB+comb predictions. Significantly narrower distributions are obtained with the QRPA+BE NLDs. Also relatively high excitation energies are needed to reach a Gaussian pattern, in contrast to assumptions made by most of the NLD formulas. For the spherical Ba isotope, the spin distribution is relatively similar to the other formulas, while for the deformed Yb isotope, the QRPA+BE spin distribution is clearly much narrower than predicted by HFB+comb model with a spin cutoff factor close to 3-4 at energies around the separation energy, as found for example by (p,p′) experiment on $^{150}$Nd isotope at these low energies [30]. Finally, note that the same calculations were performed on the basis of the D1S Gogny interaction and, qualitatively, similar results obtained for the energy, parity and spin dependences.

## 4. Comparison with experiments

The most reliable experimental data on NLD concerns the s-wave neutron resonance spacings $D_0$ at the neutron separation energy $S_n$ [2,31]. Due to the low excitation energy $S_n$ at which the level spacing can be estimated, $D_0$ is very sensitive to shell, pairing and deformation effects. The quality of a global NLD formula can be described by the root-mean-square (rms) deviation factor $f_{\rm rms}$ with respect to experimental $D_0$ values (taking the errors into account), as defined in Ref. [16].

The QRPA+BE s-wave spacings for 48 even-even nuclei are compared in Fig. 3 with experimental data [2]. An overall excellent agreement by a factor $f_{\rm rms}=1.65$ is obtained, showing the relevance of the newly proposed QRPA+BE approach to reproduce experimental data in the wide range of $74\leq A\leq 209$ globally within a factor of 2 and of no more than a factor of 3.8. This level of accuracy is similar to (or even better than) the one found by the most successful global NLD models [2]. In particular, on the same set of

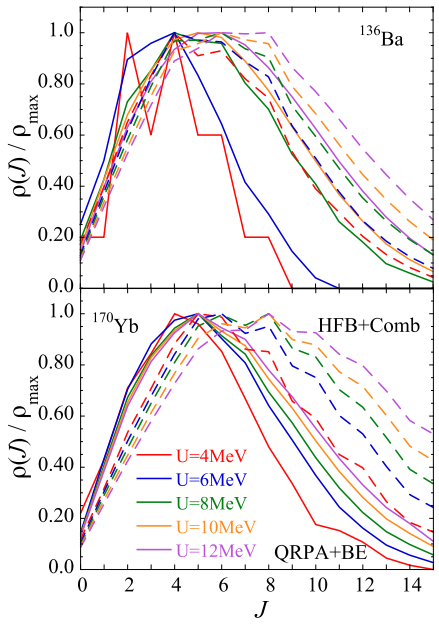


**Fig. 2.** Normalized spin distribution in the spherical $^{136}$Ba and deformed $^{170}$Yb nuclei as a function of the spin $J$ (in $\hbar$) for 5 energies between 4 and 12 MeV. The QRPA+BE spin distributions (solid lines) are compared with the HFB+comb [3] predictions (dashed lines).

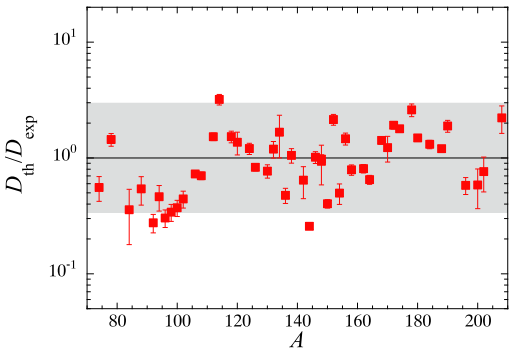


**Fig. 3.** Ratio of QRPA+BE ($D_{th}$) to the experimental ($D_{exp}$) [2] s-wave neutron resonance spacings for 48 even-even compound nuclei.

$D_0$ values, $f_{rms} = 1.5$ and 2.4 for the Cst-T and HFB+comb models, respectively. Note that the energy shift applied to the QRPA energies by $-0.15$ MeV typically reduces the NLD by a factor of 2 and the $-0.65$ MeV shift for closed-shell nuclei by a factor between 5 and 25. This simulation also shows how important it is to accurately estimate in particular the lowest QRPA energies. For this reason, this approach to NLD also represents a stringent test of the interaction used in the QRPA calculation. In particular an overestimation of the QRPA energies, for both D1S or D1M interactions, leads to an underestimate of the NLD after the boson expansion.

The energy distribution of the QRPA+BE NLD is finally compared with Oslo measurements in Fig. 4 for 9 cases using the same procedure as in Ref. [16]. QRPA+BE NLDs are seen to be in good agreement with data, even at the lowest energies in particular for $^{74}$Ge and $^{112}$Cd. The extremely complicated case of $^{208}$Pb is also seen to be relatively satisfactory and significantly better than found with traditional formulas [11,2,3].

## 5. Conclusion

To go beyond the usual particle-independent approximation, a new approach based on the boson expansion of QRPA excitations is proposed. The calculated NLDs are shown to follow an energy

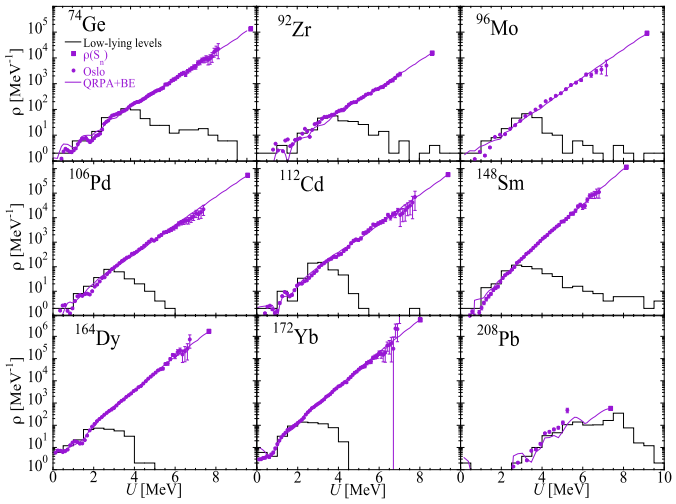


**Fig. 4.** Theoretical and renormalized Oslo NLDs for 9 even-even nuclei between $^{74}$Ge and $^{208}$Pb. The solid line represents the NLD extracted from known discrete levels on an energy bin $\Delta E = 0.5$ MeV. The solid circles correspond to the Oslo data [15] and the solid lines to the present QRPA+BE NLD predictions. The full square at $U = S_n$ corresponds to the total level density extracted for the QRPA+BE NLD model after renormalization on the experimental $D_0$ value.

dependence close to a constant-temperature formula at energies above a few MeV, but present a spin distribution that is rather narrower than what is predicted by other models, especially for deformed nuclei. The NLDs are also found to achieve equiparity at energies higher than what is obtained within the combinatorial approach. For the 48 even-even nuclei considered in the present study, a quite remarkable agreement with s-wave resonance spacings and Oslo data is found, highlighting the relevance of the present approach.

The QRPA+BE approach is restricted at the present time to even-even systems but will be in the future extended to nuclei with an odd number of nucleons. Since these systems breaks the time-reversal symmetry but also the boson nature of the QRPA excitations, they should be treated with special care. Similarly, a special attention will be given to nuclei heavier than Pb for which some truncations may need to be imposed to the QRPA calculation to remain tractable. These species will be the subject to a forthcoming study. While a long-term goal will be to improve the interaction to accurately describe the QRPA excitations, some refined systematics regarding their energy renormalisation can provide in the mean time a phenomenological approach that can further increase the accuracy of NLD predictions. A large-scale calculation of QRPA+BE NLD for applications is also foreseen in the future.

## Declaration of competing interest

The authors declare that they have no known competing financial interests or personal relationships that could have appeared to influence the work reported in this paper.

## Data availability

The authors do not have permission to share data.

## Acknowledgements

S.G. acknowledges financial support from F.R.S.-FNRS (Belgium). This work was supported by the Fonds De La Recherche Scientifique - FNRS and the Fonds Wetenschappelijk Onderzoek - Vlaanderen (FWO) under the EOS Project No O000422 and O022818F.

## References


[1] H. Bethe, An attempt to calculate the number of energy levels of a heavy nucleus, Phys. Rev. 50 (1936) 332.
[2] R. Capote, M. Herman, P. Oblozinsky, P. Young, S. Goriely, T. Belgya, A. Ignatyuk, A. Koning, S. Hilaire, V. Plujko, M. Avrigeanu, O. Bersillon, M. Chadwick, T. Fukahori, Z. Ge, Y. Han, S. Kailas, J. Kopecky, V. Maslov, G. Reffo, M. Sin, E. Soukhovitskii, P. Talou, Reference Input Parameter Library (RIPL-3), Nucl. Data Sheets 110 (2009) 3107.
[3] S. Goriely, S. Hilaire, A.J. Koning, Improved microscopic nuclear level densities within the hfb plus combinatorial method, Phys. Rev. C 78 (2008) 064307.
[4] S. Hilaire, M. Girod, S. Goriely, A.J. Koning, Temperature-dependent combinatorial level densities with the D1M gogny force, Phys. Rev. C 86 (2012) 064317.
[5] H. Uhrenholt, S. Aberg, A. Dobrowolski, T. Døssing, T. Ichikawa, P. Möller, Combinatorial nuclear level density model, Nucl. Phys. A 913 (2013) 127.
[6] T. Døssing, S. Aberg, Collective enhancements in nuclear level densities, Eur. Phys. J. A 55 (2019) 249.
[7] Y. Alhassid, M. Bonett-Matiz, S. Liu, H. Nakada, Direct microscopic calculations of nuclear level densities in the shell model monte carlo approach, Phys. Rev. C 92 (2015) 024307.
[8] Y. Alhassid, The shell model monte carlo approach to level densities: recent developments and perspectives, Eur. Phys. J. A 51 (2015) 171.
[9] V. Zelevinsky, S. Karampagia, Nulcear level density and related physics, EPJ Web Conf. 194 (2018) 01001.
[10] S. Goko, H. Utsunomiya, S. Goriely, A. Makinaga, T. Kaihori, S. Hohara, H. Akimune, T. Yamagata, Y.-W. Lui, H. Toyokawa, A.J. Koning, S. Hilaire, Partial photoneutron cross sections for the isomeric state 180tam, Phys. Rev. Lett. 96 (2006) 192501.
[11] A.J. Koning, S. Hilaire, S. Goriely, Global and local level density models and their impact on nuclear reaction calculations, Nucl. Phys. A 810 (2008) 13.
[12] P. Demetriou, S. Goriely, Microscopic nuclear level densities for practical applications, Nucl. Phys. A 695 (2001) 95.
[13] A.J. Koning, D. Rochman, Modern nuclear data evaluation with the TALYS code system, Nucl. Data Sheets 113 (12) (2012) 2841–2934, https://doi.org/10.1016/j.nds.2012.11.002.
[14] A. Koning, S. Hilaire, S. Goriely, Talys: modeling of nuclear reactions, Eur. Phys. J. A 59 (2023) 131, https://doi.org/10.1140/epja/s10050-023-01034-3.
[15] Oslo database, Level densities and gamma-ray strength functions [online], 2021.
[16] S. Goriely, A.C. Larsen, D. Mücher, Comprehensive test of nuclear level density models, Phys. Rev. C 106 (2022) 044315.
[17] P. Ring, P. Schuck, The Nuclear Many-Body Problem, Springer, 2004.
[18] S. Péru, H. Goutte, Role of deformation on giant resonances within the qrpa approach and the gogny force, Phys. Rev. C 77 (2008) 044313.
[19] S. Péru, G. Gosselin, M. Martini, M. Dupuis, S. Hilaire, J.-C. Devaux, Giant resonances in u238 whithin the quasi-particle random-phase approximation with the gogny force, Phys. Rev. C 83 (2011) 014314.
[20] S. Péru, M. Martini, Mean field based calculations with the gogny force: some theoretical tools to explore the nuclear structure, Eur. Phys. J. A 50 (2014) 88.
[21] M. Martini, S. Péru, S. Hilaire, S. Goriely, F. Lechaftois, Large-scale deformed qrpa calculations of the gamma-ray strength function using the gogny force, Phys. Rev. C 94 (2016) 014304.
[22] S. Goriely, S. Hilaire, S. Péru, M. Martini, I. Deloncle, F. Lechaftois, The gogny-hfb+qrpa predictions of the $m1$ strength function and its impact on radiative neutron capture cross section, Phys. Rev. C 94 (2016) 044306.
[23] I. Deloncle, S. Péru, M. Martini, Electromagnetic dipole and gamow-teller responses of even and odd 90-94zr isotopes in qrpa calculations with the d1m gogny force, Eur. Phys. J. A 53 (2017) 170.
[24] S. Goriely, S. Hilaire, M. Girod, S. Péru, First gogny hatree-fock-bogoliubov nuclear mass model, Phys. Rev. Lett. 102 (2009) 242501–242504.
[25] S. Goriely, S. Hilaire, S. Péru, K. Sieja, Gogny-HFB+QRPA dipole strength function and its application to radiative nucleon capture cross section, Phys. Rev. C 98 (2018) 014327.
[26] M. Martini, S. Péru, S. Goriely, Gamow-teller strength in deformed nuclei within the self-consistent charge-exchange quasiparticle random-phase approximation with the gogny force, Phys. Rev. C 89 (2014) 044306.
[27] S. Hilaire, J.-P. Delaroche, M. Girod, Combinatorial nuclear level densities based on the gogny nucleon-nucleon effective interaction, Eur. Phys. J. A 12 (2001) 169.
[28] S. Hilaire, S. Goriely, Global microscopic nuclear level densities within the hfb plus combinatorial method for practical applications, Nucl. Phys. A 779 (2006) 63.
[29] T. Døssing, A. Jensen, Nuclear level densities with collective rotations included, Nucl. Phys. A 222 (1974) 493.
[30] M. Guttormsen, K.O. Ay, M. Ozgur, E. Algin, A.C. Larsen, F.L. Bello Garrote, H.C. Berg, L. Crespo Campo, T. Dahl-Jacobsen, F.W. Furmyr, D. Gjestvang, A. Görgen, T.W. Hagen, V.W. Ingeberg, B.V. Kheswa, I.K.B. Kullmann, M. Klintefjord, M. Markova, J.E. Midtbø, V. Modamio, W. Paulsen, L.G. Pedersen, T. Renstrøm, E. Sahin, S. Siem, G.M. Tveten, M. Wiedeking, Evolution of the $\gamma$-ray strength function in neodymium isotopes, Phys. Rev. C 106 (2022) 034314, https://doi.org/10.1103/PhysRevC.106.034314, https://link.aps.org/doi/10.1103/PhysRevC.106.034314.
[31] S. Mughabghab, Atlas of Neutron Resonances: Resonance Parameters and Thermal Cross Sections. Z= 1-100, Elsevier, 2006.